Analytica Chimica Acta 787 (2013) 193–202

Contents lists available at SciVerse ScienceDirect

Analytica Chimica Acta

journal homepage: www.elsevier.com/locate/aca

In vivo imaging of the morphology and changes in pH along the gastrointestinal tract of Japanese medaka by photonic band-gap hydrogel microspheres

Xuemin Du[a,b,c], Ngai-Yu Lei[c], Peng Hu[c], Zhang Lei[d], Daniel Hock-Chun Ong[d], Xuewu Ge[a,b], Zhicheng Zhang[a,b,**], Michael Hon-Wah Lam[a,c,*]

[a] *Advanced Laboratory for Environmental Research & Technology, USTC-CityU, Suzhou 215123, China*
[b] *Department of Polymer Science and Engineering, University of Science & Technology of China, Hefei, Anhui 230026, China*
[c] *Centre for Functional Photonics, Department of Biology and Chemistry, City University of Hong Kong, Tat Chee Avenue, Kowloon, Hong Kong, China*
[d] *Department of Physics, The Chinese University of Hong Kong, Shatin, Hong Kong, China*

HIGHLIGHTS

- Fabrication of pH-responsive photonic colloidal crystalline microspheres.
- Specific photonic band-gap responses occurred in the pH range of 4–5.
- Remarkably low *in vivo* toxicity to Japanese medaka (*Oryzia latipes*).
- *In vivo* imaging of the morphology and pH along GI tract of Japanese medaka.
- Demonstrates bio-imaging potentials of stimuli-responsive photonic materials.

GRAPHICAL ABSTRACT

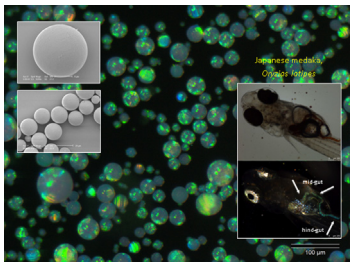

ARTICLE INFO

Article history:
Received 5 March 2013
Received in revised form 6 May 2013
Accepted 8 May 2013
Available online 20 May 2013

Keywords:
Photonic band-gap microspheres
In vivo imaging
Gastrointestinal tract
Japanese medaka
pH-responsive

ABSTRACT

Colloidal crystalline microspheres with photonic band-gap properties responsive to media pH have been developed for *in vivo* imaging purposes. These colloidal crystalline microspheres were constructed from monodispersed core–shell nano-size particles with poly(styrene-*co*-acrylic acid) (PS-*co*-PAA) cores and poly(acrylic acid-*co*-*N*-isopropylacrylamide) (PAA-*co*-PNIPAM) hydrogel shells cross-linked by *N*,*N*′-methylenebisacrylamide. A significant shift in the photonic band-gap properties of these colloidal crystalline microspheres was observed in the pH range of 4–5. This was caused by the discontinuous volume phase transition of the hydrogel coating, due to the protonation/deprotonation of its acrylic acid moieties, on the core–shell nano-sized particles within the microspheres. The *in vivo* imaging capability of these pH-responsive photonic microspheres was demonstrated on a test organism – Japanese medaka, *Oryzia latipes* – in which the morphology and change in pH along their gastrointestinal (GI) tracts were revealed under an ordinary optical microscope. This work illustrates the potential of stimuli-responsive photonic band-gap materials in tissue-/organ-level *in vivo* bio-imaging.

© 2013 Elsevier B.V. All rights reserved.

* Corresponding author at: Centre for Functional Photonics, Department of Biology and Chemistry, City University of Hong Kong, Tat Chee Avenue, Kowloon, Hong Kong, China. Tel.: +852 34427329; fax: +852 34420522.
** Corresponding author at: Department of Polymer Science and Engineering, University of Science & Technology of China, Hefei, Anhui 230026, China.
E-mail addresses: zczhang@ustc.edu.cn (Z. Zhang), bhmhwlam@cityu.edu.hk, michaellam1964@gmail.com (M.H.-W. Lam).

0003-2670/$ – see front matter © 2013 Elsevier B.V. All rights reserved.
http://dx.doi.org/10.1016/j.aca.2013.05.022

1. Introduction

In vivo imaging, the non-invasive visualization of histo/cytochemical and metabolic events, as well as specific pathological conditions, within whole organisms, is one of the key developments in molecular medicine [1]. Besides the more traditional radiological techniques, such as magnetic resonance imaging (MRI) and positron emission tomography (PET), optical *in vivo* imaging is gaining increasing attentions in recent years. This is perhaps because of their comparatively simpler instrumental requirements, rapid acquisition time, and capability of achieving ultra-high image resolution [2]. Numerous strategies, such as the tagging of designated antibodies, analyte-receptors, and analyte-responsive molecular functionalities onto optical imaging probes, have been developed for the recognition of *in vivo* targets, or to respond to selected metabolic activities in specific tissues with relevant physiological conditions [3]. At present, most of the *in vivo* imaging probes are based either on organic- and coordination molecular luminophores [4], or nanoparticles, such as dye-doped colloidal nanoparticles, lanthanide-based nanoparticles and quantum dots [5]. Other non-luminescent materials, such as nanogold particles, have also been explored [5h,6]. Nevertheless, one of the major concerns that encumbered their genuine biomedical applications, such as diagnostic imaging on patients, is their inherent cyto- and *in vivo* toxicity [7]. New optical imaging strategies that can do without the use of potentially toxic chemicals are attractive alternatives that are deemed worthy of exploring.

Photonic band-gap materials constructed from three-dimensional arrays of highly ordered, periodically packed nano-sized particles possess intriguing ability to manipulate light in the UV, visible and near-IR (NIR) spectral range. They have rapidly aroused interests from researchers in fields of optics and opto-electronics, as well as chemosensing [8]. Photonic band-gap properties of these materials are originated from the Bragg diffraction of UV, visible and NIR radiation by the orderly packed lattices of nano-sized particles and offer desirable features such as: (a) no chemical chromophores/fluorophores are required; (b) bio-compatible, biodegradable materials can be used to construct the photonic lattices so as to ensure their safety for biomedical applications; (c) convenient tunability of photonic band-gap properties by adjusting the size of the particles that assembled the photonic lattices; (d) fully compatible with optical microscopy with minimal interference from samples (no need of photo-excitation, and hence, no background autofluorescence and photo-bleaching); (e) specific functional moieties can be easily incorporated so that photonic band-gap properties can be responsive towards targeted analytes, or physiological conditions. Despite these attractive features, report on the application of photonic band-gap materials in bio-imaging is scarce. To prove the feasibility of this idea, we developed a set of hydrogel-based photonic band-gap microspheres that can respond primarily to physiological pH changes and used them to image the lumenal pH of the gastrointestinal tract of a freshwater vertebrate model organism – Japanese medaka (*Oryzias latipes*). Monitoring of the acid–base balance at the tissue and organ level is important as many pathological states, such as inflammation, ischaemia, and cancers, are associated with systemic acid–base imbalance [9]. Despite this importance, there is a general lack of clinical tool for the *in vivo* imaging of the spatial distribution of pH [10].

Majority of the literature-reported stimuli-responsive photonic band-gap materials for chemosensing applications are in the form of polymerized colloidal crystal array (PCCA) thin-films [11]. While this configuration facilitates spectroscopic measurement of sensing responses, PCCA thin-films may not be very compatible with *in vivo* sensing and imaging. Numerous recent works on photonic band-gap materials have reported spherical supraballs of relatively large diameter (>100 μm) that displayed interesting photonic phenomena [12]. A suite of novel techniques, such as water/air interface evaporation, electrospraying, ink-jet printing, and microfluidic droplet-extrusion, have been developed for the fabrication of photonic beads of various size [13]. In this work, we designed and fabricated pH-responsive colloidal crystalline photonic microspheres *via* the three-dimensional orderly packing of monodispersed core–shell nano-sized particles by a wet self-assembly technique (Scheme 1) [14]. These core–shell nano-sized particles were specially designed to bear a poly(styrene-*co*-acrylic acid) (PS-*co*-PAA) core and a slightly cross-linked poly(acrylic acid-*co*-*N*-isopropylacrylamide) (PAA-*co*-PNIPAM) co-polymer hydrogel shell. Critical solution temperatures (CSTs) of hydrogels generated from hydrophilic acrylic acid and *N*-isopropylacrylamide are well known to be dependent on the media pH, ionic strength and temperature [15]. Deprotonation of the carboxylic functionality of the acrylic acid component within those hydrogels can bring about their discontinuous Donnan osmotic swelling [16]. In this case, the volume phase transition of the cross-linked PAA-*co*-PNIPAM hydrogel shells of the nano-sized particles perturbs the photonic band-gap properties of their assembled microspheres.

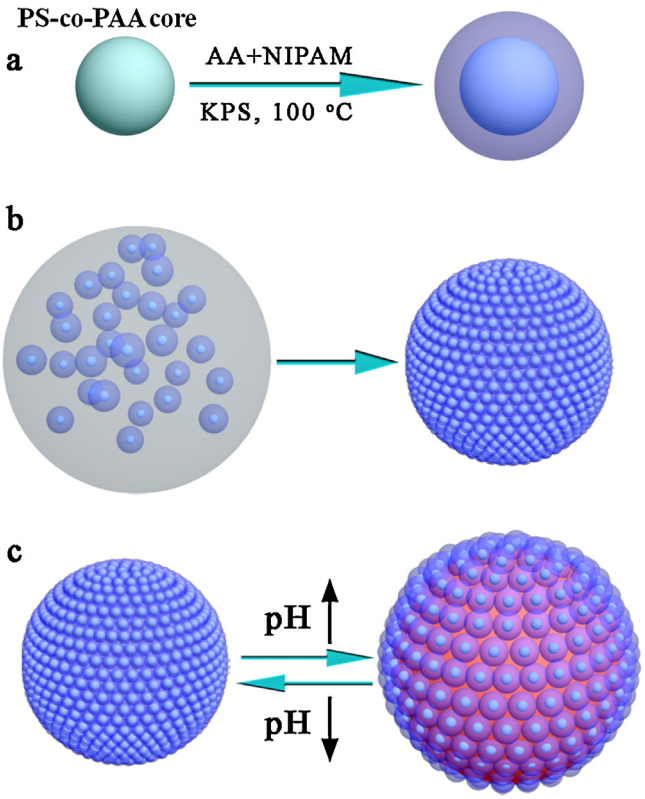

Scheme 1. Schematic illustration of the colloidal crystalline microspheres: (a) the preparation of the hydrogel core–shell nano-sized particles; (b) the assembly of the core–shell particles into microspheres by the wet self-assembly technique; (c) mechanism of the photonic band-gap responses of the hydrogel microspheres to the media pH.

2. Experimental

2.1. Materials

Styrene, divinylbenzene, acrylic acid, potassium persulfate and all the organic solvents were purchased form Aldrich. *N*-isopropylacrylamide (NIPAM), and *N,N′*-methylenebisacrylamide were purchased from Acros. Hypermer 2296 was purchased

from Croda. All chemicals, except styrene, were used as received without further purification. Styrene was purified by treating with 5 wt% aqueous NaOH to remove the inhibitor.

2.2. Materials characterization

Scanning electron microscopy (SEM) and transmission electron microscopy (TEM) were carried out on a Philips XL30 ESEM-FEG environmental scanning electron microscope, and a FEI/Philips Tecnal 12 Bio TWIN transmission electron microscope respectively. Photographs of the microspheres were taken with an optical microscope (Olympus BX60 and Nikon Eclipse 90i) equipped with CCD camera (Media Cybernetics Evolution MP 5.0 and SPOT Xplorer, respectively). Microspheres were illuminated by white light focused through an objective (20×, NA = 0.40) onto the samples. UV–vis reflectance spectra of the microspheres in the range 400–750 nm were measured using the optical microscope (Olympus BX60, 20×, NA = 0.40) that was fitted to a SpectraPro 2300i spectrometer (Princeton Instrument) *via* an optical lens and a light guide. A Leica M205 FA motorized fluorescence stereomicroscope, equipped with a DCF 310 FX CCD camera, was used for the microscope imaging of Japanese medaka, *O. latipes*. Dynamic light scattering measurements were carried out with a Malvern Zetasizer Nano ZS instrument at 25 °C.

2.3. Preparation of core–shell nano-sized particles

The hydrogel core–shell nano-sized particles were prepared by the seeded copolymerization of acrylic acid and *N*-isopropylacrylamide with the poly(styrene-*co*-acrylic acid) (PS-*co*-PAA) cores as seed particles using potassium persulfate as an initiator in accordance with literature method [17] with slight modification. Styrene (5.5 g, 53 mmol), divinylbenzene (0.55 g, 4.2 mmol) and acrylic acid (0.63 g, 8.8 mmol) were mixed in 100 mL of deionized water in a 250 mL round-bottom flask, and the resultant mixture was mechanically and warmed to 100 °C. Polymerization was initiated by the addition of 63 mg (0.2 mmol) of potassium persulfate in 5 mL of deionized water. The polymerization process was allowed to proceed for 2 h for the formation of the PS-*co*-PAA seed particles. Then, 10 mL of an aqueous solution containing *N*-isopropylacrylamide (1.0 g, 8.8 mmol), acrylic acid (3.0 g, 42 mmol), *N,N′*-methylenebisacrylamide (130 mg, 840 nmol) and potassium persulfate (24 mg, 0.09 mmol) were added to the resultant mixture. Polymerization was allowed to proceed for another 3 h to produce the hydrogel core–shell particles, which were isolated and purified by centrifugation at 15,500 rpm for 3 × 20 min to remove the excess reagents and water-soluble oligomers.

Two additional sets of core–shell nano-sized particles with lower content of *N,N′*-methylenebisacrylamide cross-linker in the hydrogel coating have also been fabricated. These nano-sized particles were prepared in a similar way as described above except that the *N,N′*-methylenebisacrylamide used was 12 mg and 24 mg respectively. Core–shell nano-sized particles without the acrylic acid functional moiety in the hydrogel shells were also prepared in similar way as described above, except that no acrylic acid was used in the fabrication of the coating.

2.4. Fabrication of the colloidal crystalline microspheres

An aqueous suspension (1 mL) of the core–shell nano-sized particles (at a loading of 4.0 wt%) was dropped into 15 mL of hexadecene containing 2.0 wt% of an amphiphilic block co-polymer, Hypermer 2296, as a stabilizer. The aqueous suspension was emulsified in the organic solvent by vigorous shaking, and was then poured into a glass petri dish, of which the glass surface had been rendered hydrophobic by chemical modification with octadecyltrichlorosilane. The emulsified mixture was kept at 50 °C for 72 h. The colloidal crystalline microspheres were formed as water in the emulsified droplets evaporated and left behind closely packed lattices of core–shell particles. These colloidal crystalline microspheres were collected by centrifugation at 3000 rpm for 1 min, followed by washing with *n*-hexane to remove hexadecene. The *n*-hexane was then removed by freeze-drying to obtain the microspheres as a light blue powder designated as R3 microspheres.

Two additional sets of photonic colloidal crystalline microspheres have also been constructed from core–shell nano-sized particles with lower content of *N,N′*-methylenebisacrylamide cross-linker. They were prepared in a similar way as the R3 microspheres above, with the exception that core–shell nano-sized particles fabricated with 12 mg (R1 microspheres) and 24 mg (R2 microspheres) of *N,N′*-methylenebisacrylamide were used. Control photonic colloidal crystalline microspheres that were not responsive to media pH were fabricated in a similar way as described above, except that core–shell nano-sized particles without acrylic acid functional moiety in the hydrogel shells were used instead.

2.5. Measurement of reflectance spectra of the colloidal crystalline microspheres

The colloidal crystalline microspheres (control and R3 microspheres) were suspended in aqueous buffers of pre-determined pH and ionic strength. The suspensions were dropped into the wells of depression microscope slides, which were then covered with cover slips and were immediately used for microscopy observation, photography and measurement of reflectance spectra. Low magnification power (20×) was used to ensure that averaged spectral characteristics of a collection of microspheres were measured instead of any specific individual particles. All measurements were carried out at room temperature, *i.e.* 25 °C.

2.6. In vivo imaging of Japanese medaka, Oryzias latipes

Medaka embryos were obtained from Dr. Doris W.T. Au (City University of Hong Kong). Hatched larvae were maintained in an embryo rearing medium [18], at pH 7.2, and fed with finely ground Otohime BETA1 (Nisshin Co., Japan). Larvae (*ca.* 4–5 mm in length) were fasted for 5 h and then exposed to the colloidal crystalline microspheres at 5 day-post-hatch (dph) on multiwell cell culture plates. In each of the cell culture well, two medaka larvae (5-dph) were incubated in 3 mL of embryo rearing medium, with a suspension of 1.0 mg of colloid crystalline microspheres (pH-responsive photonic microspheres or control microspheres), for 24 h. The larvae were then transferred into the well of depression microscope slides and turned so that their dorsal side was faced upward, with the help of a dropper, for microscope imaging. RGB values of selected areas on captured images were measured with Photoshop CS2.

2.7. In vivo toxicity assay

Larvae (*ca.* 4–5 mm in length) were fasted for 5 h and then exposed to the colloidal crystalline microspheres at 5 day-post-hatch (dph) on multiwell cell culture plates. Five medaka larvae were held in each of the cell culture well. These larvae was incubated in 7 mL of embryo rearing medium, at room temperature, with a suspension of the colloidal crystalline microspheres of known concentration from 0 to 10 mg mL^{-1}, and were fed every other day, continuously for up to 7 days. Their vitality was checked every 24 h. Data processing refers to the software of SPSS 17.0.

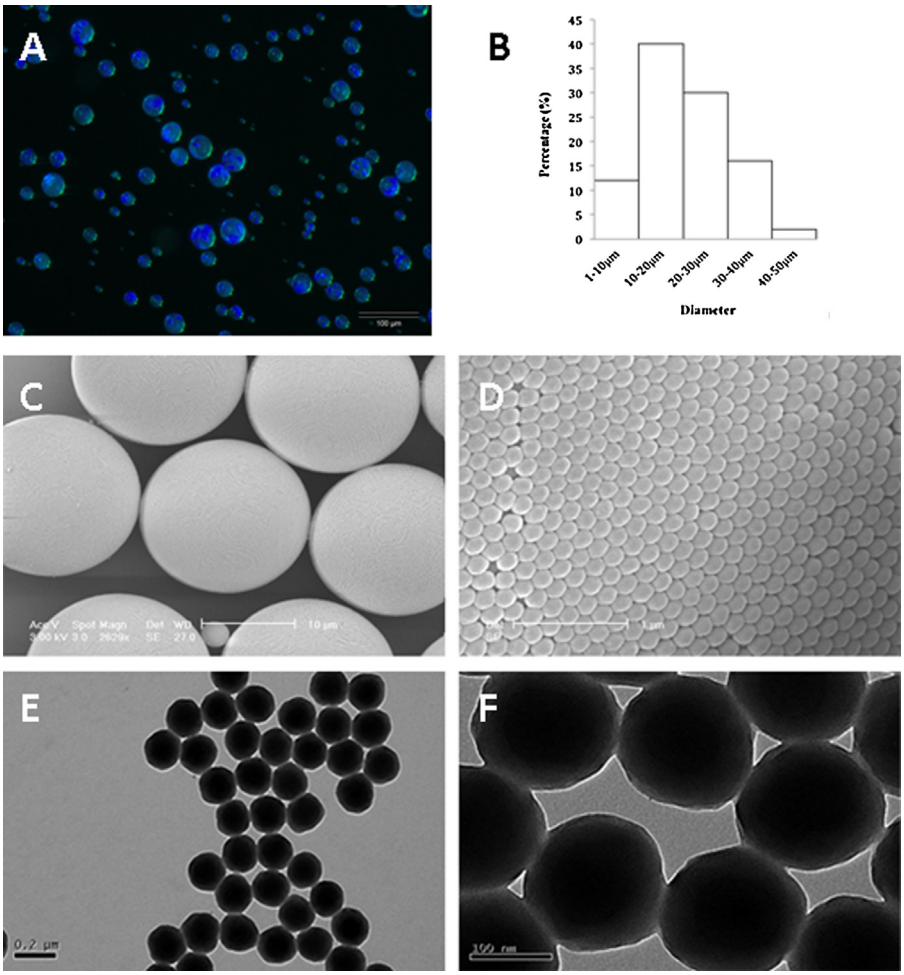

Fig. 1. The colloidal crystalline microspheres: (A) a typical image of an aqueous suspension (pH = 3.3) of the microspheres under an optical microscope illuminated by white light focused through the objective (20×, NA = 0.40); (B) size distribution of the microspheres obtained by optical microscopy; (C) a typical SEM image of the microspheres; (D) a close-up SEM image of a microsphere showing the orderly packed nano-sized particles; (E) and (F) TEM images of the monodispersive core–shell particles of diameter *ca.* 170 nm.

3. Results and discussion

Fig. 1 shows the optical microscope, SEM and TEM images of the core–shell nano-sized particles, as well as the assembled colloidal crystalline microspheres. From the TEM images, the core–shell nano-sized particles were monodispersed with a diameter of *ca.* 170 nm. On the other hand, the assembled microspheres were more polydispersed, with particle diameter ranging from <10 μm to 50 μm. About 40% of the microspheres were in the 10–20 μm range. The actual size of the core–shell particles and the microspherical assemblies in aqueous buffers are expected to be larger (Fig. 1A) because of the swelling properties of their hydrogel shells. Dynamic light scattering measurement of the PS-*co*-PAA cores and the resultant core–shell nano-sized particles suspended in an acetate buffer of pH 3 revealed their hydrodynamic diameters to be 209 ± 2 nm and 235 ± 4 nm, respectively. This suggests that the thickness of the PAA-*co*-PNIPAM hydrogel coating on the core–shell nano-sized particles is *ca.* 13 nm. The polydispersity index (PDI) of the core–shell particles suspended in the acidic aqueous buffer was 0.009.

Photonic band-gap properties of the colloidal crystalline microspheres can be described in a similar way as photonic PCCA thin-films by a combination of the Bragg's and Snell's law [19]:

$$\lambda_{\max} = 1.633\frac{d}{m}\sqrt{\sum n_i^2 V_i - \sin^2\theta} \quad (1)$$

where $\lambda_{\max}$ is the wavelength of the diffraction peak; d is the diameter of the hydrogel particles that assembled the orderly packed lattice; m is the order of the Bragg diffraction; n_i and V_i are the refractive index and the volume fraction of the ith component of the overall microspherical assembly; and θ is the angle measured from normal incident. Assuming that: (a) the hydrogel core–shell particles adopted a face-centred cubic (*fcc*) close packing within the assembled microspheres, (b) the diameter of the hydrogel core–shell particles suspended in the aqueous media was 235 nm, and (c) the relative composition of PS, PAA and PNIPAM in the hydrogel nano-sized particles were equivalent to the mole ratio of their corresponding monomers, *i.e.* 6:5.6:1 (PS:PAA:PNIPAM), the $\lambda_{\max}$ of the hydrogel photonic microspheres is estimated to be 545 nm at ambient temperature below the lower critical solution temperature (LCST) of PNIPAM (*i.e.* <34 °C) [20], and at $\theta = 0$. Fig. 2 shows the UV–vis reflectance spectra of the colloidal crystalline microspheres in aqueous media buffered at various pH from 3.3 to 11.0. Without any addition of NaCl, the ionic strength of the media was maintained in the range of 5.0 mM (pH 3.3) to 10.4 mM (pH 11.0) by the titration of 5.0 mM of acetic acid with 1.0 M NaOH for pH adjustment. At lower media pH (pH ≤ 4.0), the diffraction $\lambda_{\max}$ was observed at *ca.* 520 nm, which was close to the estimated λ_{max} according to Eq. (1). As the media pH increased, a radical change in the photonic band-gap properties of the hydrogel microspheres was observed between pH 4.0 and pH 5.0. The Bragg diffraction $\lambda_{\max}$ shifted from *ca.* 520 nm to *ca.* 620–670 nm at higher pH (pH ≥ 5.0).

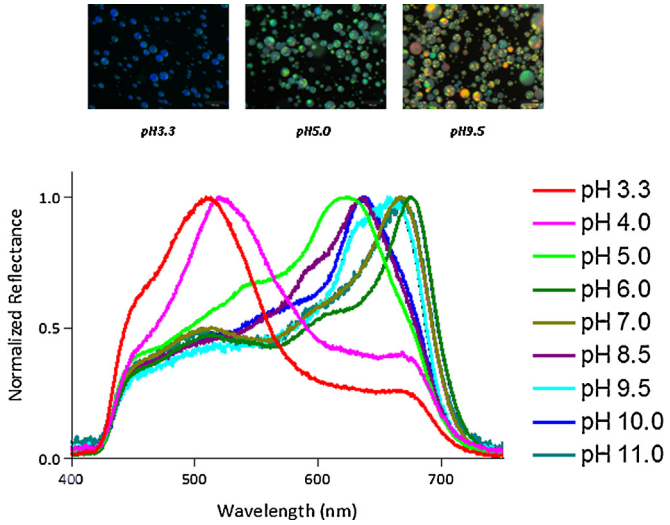

Fig. 2. Normalized reflectance spectra of the colloidal crystalline microspheres at various media pH maintained *via* the direct adjustment of concentrations of acetic acid and NaOH. No NaCl was added to the media. Photonic band-gap properties of the microspheres at selected media pH were recorded by photography (inserts above the spectra).

Such a significant red-shift of the photonic band-gap properties can be attributed to the volume phase transition of the PAA-*co*-PNIPAM hydrogel shells of the core–shell particles within the microspheres, due to the deprotonation of the carboxylic functional groups in the hydrogel. Subsequent osmotic swelling of their hydrogel shells increased the effective diameter of the particles and shifted the λ_{max} towards longer wavelength. The pK_a value of the carboxylic group of acrylic acid is 4.4 [21]. This corresponds well with the volume phase transition behaviour of the PAA-*co*-PNIPAM hydrogel shell.

Other than pH, ionic strength of the media also contributes significantly to the osmotic swelling of hydrogels [22]. In general, an increase in the ionic strength of the aqueous media causes hydrogels to shrink in volume. Thus, the photonic band-gap properties of an *in vivo* bio-imaging agent for pH may be interfered by the fluctuation of ionic strength in the *in vivo* microenvironments of the subject organism. To minimize such interference, a cross-linker, *N,N′*-methylenebisacrylamide was used in the fabrication of the PAA-*co*-PNIPAM hydrogel shell of the nano-sized particles. *N,N′*-Methylenebisacrylamide is a cross-linker commonly used in the fabrication of polyacrylamide hydrogels for gel electrophoresis and other biomedical/bioanalytical applications. It can cross-link the linear polymeric strains in the PAA-*co*-PNIPAM hydrogel to form a three-dimensional polymer network with much higher physical strength against osmotic swelling. The inability of the cross-linked polymer strains within the hydrogel material to move apart upon uptake of water builds up pressure potential within the hydrogel to oppose the further influx of water. Resistance of the hydrogel shell of the nano-sized particles to osmotic swelling increases with the degree of cross-linking, *i.e.* the amount of cross-linker used. Of course, a balance has to be struck as the resultant photonic microspheres might lose their capability of responding to media pH change as well if the degree of cross-linking is too high. In this study, we have chosen a loading of cross-linker of 2 mol% with respect to acrylic acid in the hydrogel. In order to illustrate the effect of such a cross-linked hydrogel coating on the photonic band-gap properties of the colloidal crystalline microspheres at different media ionic strength, two additional sets of microspheres with only 0.2 and 0.4 mol% of the cross-linker, with respect to acrylic acid, were fabricated. There were designated R1 and R2, while the colloidal crystalline microspheres adopted for *in vivo* imaging throughout this work was designated R3. Fig. 3 shows the photonic band-gap properties of these microspheres in aqueous buffers of pH 7.0 with different media ionic strengths. The addition of 38.5 mM, 77.0 mM and 154 mM of NaCl to the buffer solutions mimicked the physiological condition of 1/4-, 1/2- and full isotonic strength (*i.e.* 0.9% NaCl). With 0.2 and 0.4 mol% of cross-linkers, only very weak photonic Bragg diffraction of longer wavelength radiation (red and orange yellow in colour) was observable from

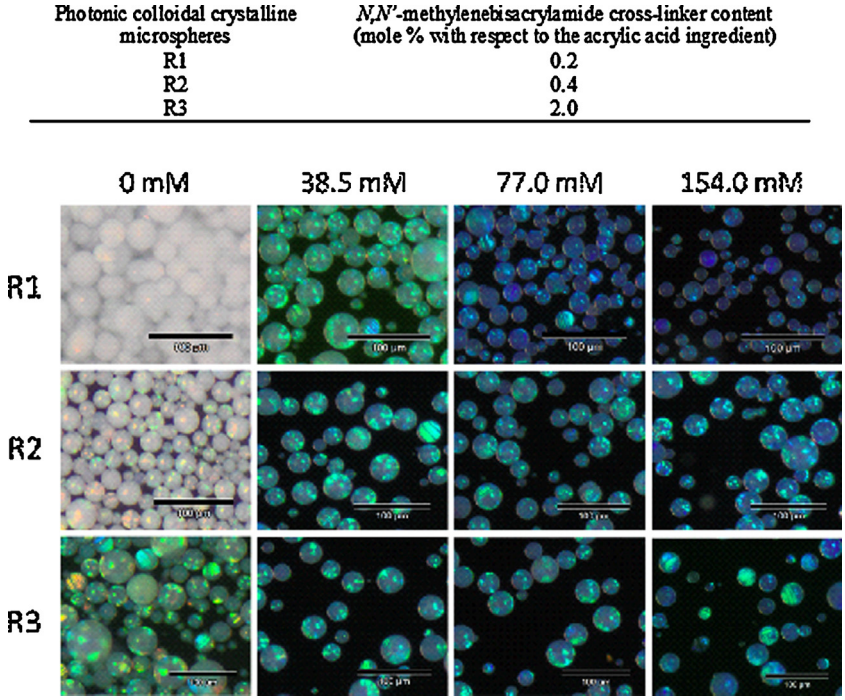

Fig. 3. Effect of cross-linker content within the hydrogel coating of the core–shell nano-sized particles on the photonic band-gap responses of the resulting colloidal crystalline microspheres to media ionic strength. Ionic strength of the aqueous buffer (pH = 7.0) was adjusted by the addition of NaCl.

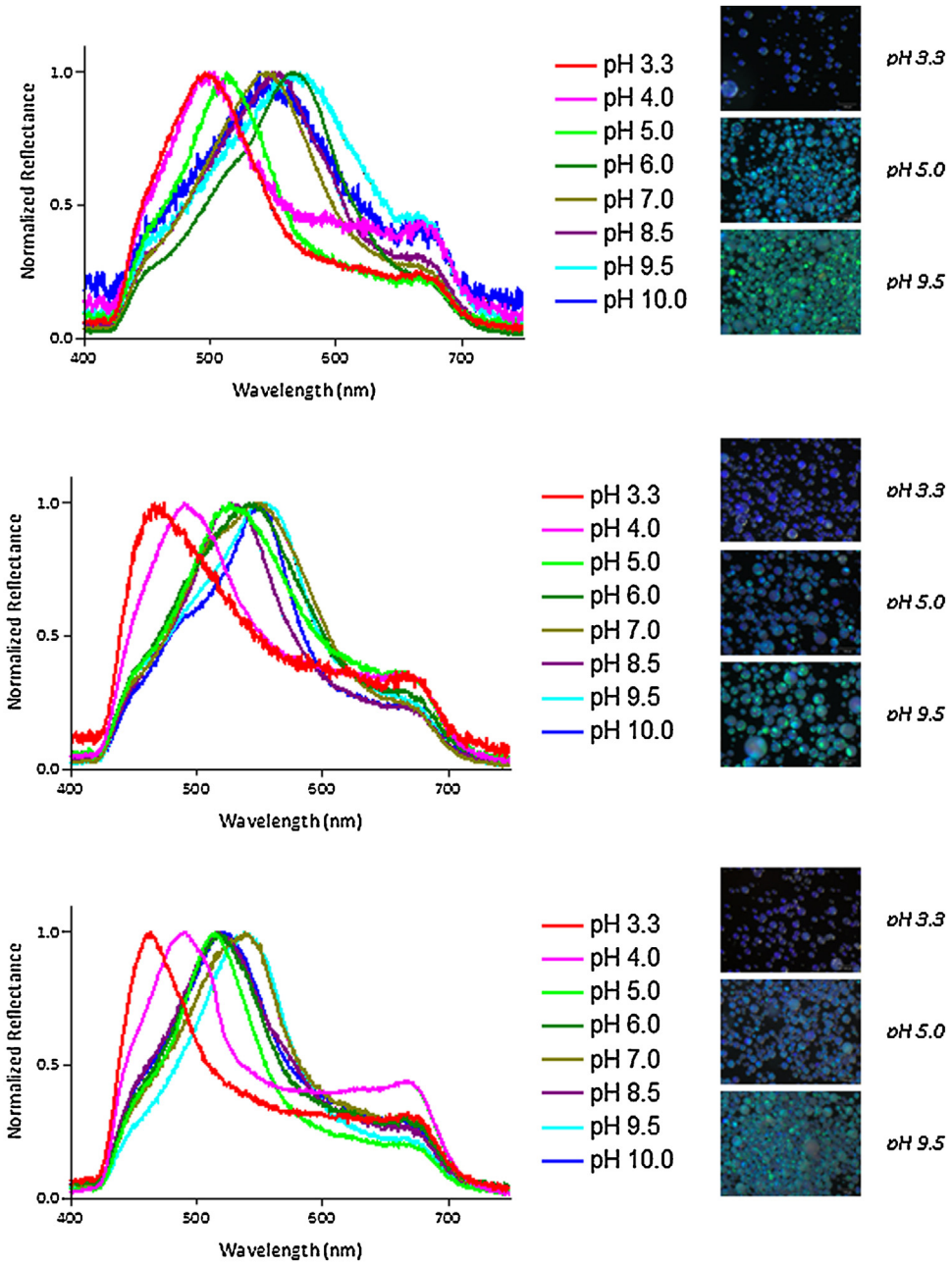

Fig. 4. Normalized reflectance spectra of the colloidal crystalline microspheres (R3 microspheres) at various media pH and ionic strengths obtained *via* the addition of 38.5 mM (A), 77.0 mM (B) and 154.0 mM (C) of NaCl to the buffer solutions. Photonic band-gap properties of the microspheres at selected media pH were recorded by photography (inserts next to the spectra).

the microspheres at low media ionic strength. This is probably due to the extensive osmotic swelling, and softening of their nano-sized particles that rendered them difficult to adopt any high-degree orderly packing. At higher media ionic strengths, shrinking of the nano-sized particles brought the photonic Bragg diffraction colour of the microspheres to the green to indigo range. Such a drastic shift in photonic properties with media ionic strength is not desirable for *in vivo* pH imaging. On the other hand, at a cross-linker content of 2.0 mol%, the hydrogel coating on the nano-sized particles was able to restrain its swelling and shrinking behaviour with media ionic strength fluctuating within the physiological range. From a quarter to full isotonic strength at pH 7.0, photonic band-gap properties of the R3 microspheres remained in the blue-green colour range. Fig. 4 shows the UV–vis reflectance spectra of the R3 microspheres at various media pH and ionic strengths. At higher media ionic strength, the extent of osmotic swelling of the hydrogel shell of the core–shell particles was reduced. This was evidenced in the photonic band-gap properties of the microspheres. At lower buffer pH (pH < 5.0), diffraction λ_{max} shifted from *ca.* 520 nm in the case of neat acetic acid/NaOH buffer to *ca.* 460–510 nm. At higher buffer pH (pH > 5.0), diffraction λ_{max} were observed at *ca.* 550–580 nm instead of *ca.* 620–670 nm in neat buffers without the addition of NaCl. Nevertheless, throughout the range of media ionic strengths, the volume phase transition of the hydrogel coating that bring about the visual shift of the photonic Bragg diffraction colour from indigo at lower pH to green at higher pH, of the microspheres was still observed between pH 4.0 and pH 5.0. As a consequent, the R3 colloidal crystalline microspheres were used in all of the

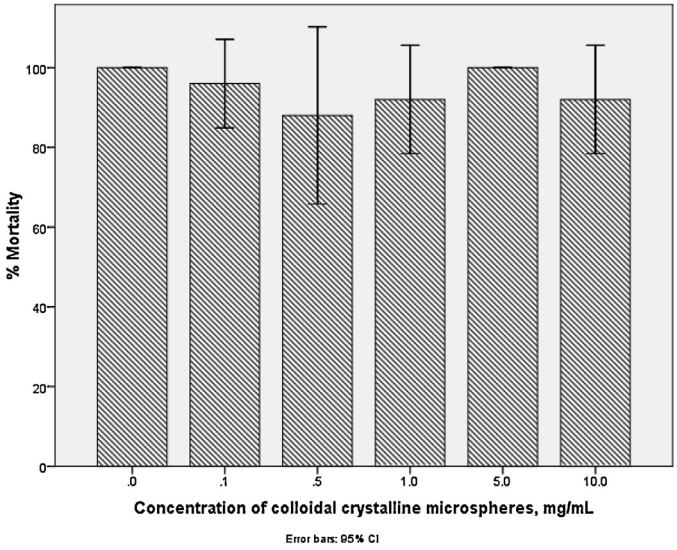

Fig. 5. *In vivo* toxicity studies of the colloidal crystalline microspheres on Japanese medaka. Larvae were exposed to culture medium with different concentration of the microspheres from 0 to 10.0 mg mL^{-1}, and were fed once every other day, continuously for up to 7 days.

in vivo imaging experiments. Control microspheres from similar core–shell nano-sized particles but contained no acrylic acid in their hydrogel coating have also been fabricated. With the same degree of cross-linking in the hydrogel coating on the nano-sized particles within these microspheres, their photonic band-gap properties were very similar to the R3 microspheres, with the exception of a lack of response to changes in the media pH. These control microspheres were used alongside with the responsive microspheres in our *in vivo* imaging experiments.

In fish physiology, the gut morphology and pH are usually determined by dissection and direct pH measurement using micro pH probes [23]. However, for fish species of very small size, *e.g.* zebrafish and Japanese medaka, which have been extensively used as vertebrate model organisms in biomedical and pharmaceutical studies [24], this could be a very difficult task. Rønnestad et al. [25] adopted a tedious and invasive method of manually injecting colorimetric pH indicator solutions into the gut compartments of Japanese flounder, *Paralichthys olivaceus*, larvae to study the functional ontogeny of their digestive tracts. To the best of our knowledge, there is no detail measurement of the lumenal pH along the GI tract of *O. latipes*. Here, we applied the pH-responsive colloidal crystalline photonic band-gap microspheres (R3 microspheres) to image the morphology and changes of lumenal pH along the gastrointestinal (GI) tract of live Japanese medaka (*O. latipes*) using an ordinary optical microscope. Medaka larvae (*ca.* 4–5 mm in length) were kept in the embryo-rearing medium in six-well cell culture plate, and were fed with the pH-responsive R3 photonic colloidal crystalline microspheres, as well as the control microspheres. The relatively low specific gravity, with respect to water, of the polystyrene-polyacrylic acid-based colloidal crystalline microspheres allowed these microspheres to suspend in the embryo-rearing medium rather than rapidly sunk to the bottom of the wells. Once introduced, the fish larvae actively fed on these microspheres. Accumulation of these photonic materials in the GI tract was observed within 24 h. Excretion of the microspheres was also observed. No abnormal behaviour, nor mortality, of the fish was ever observed within the 7-days exposure period (Fig. 5). These microspheres passed through the GI tract of *O. latipes* without causing any apparent adverse effect to the organism. Furthermore, photonic band-gap properties of both the pH-responsive and

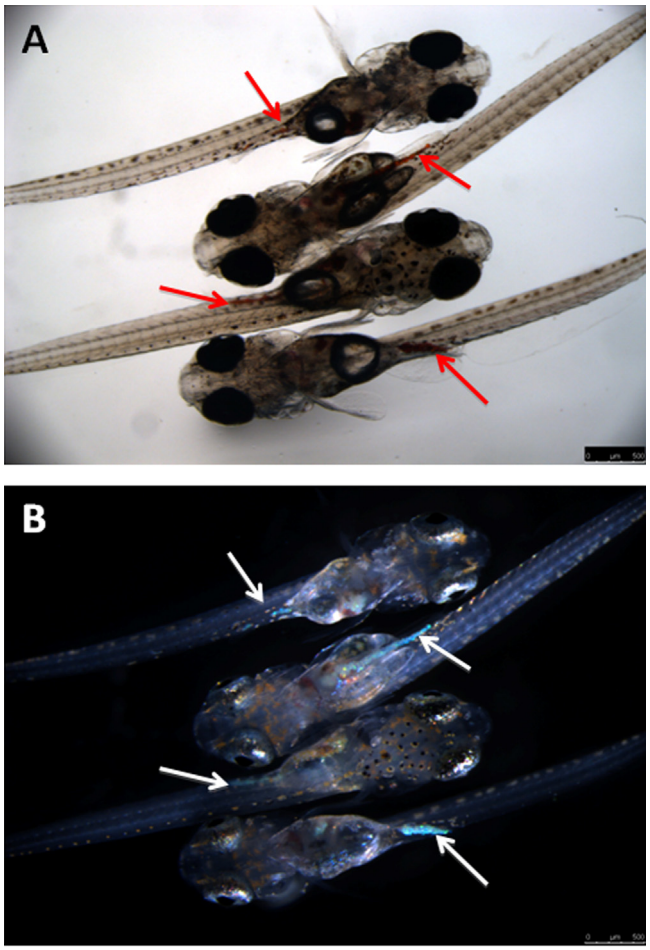

Fig. 6. Optical microscopy images of live Japanese medaka (*Oryzias latipes*) exposed to the colloidal crystalline microspheres (R3 microspheres) in the culture media for 24 h. Both bright-field (A) and dark-field (B) images show the accumulation of the microspheres in the gastrointestinal tract (more obvious at the rear end). The dark-field image also demonstrates that specific photonic band-gap properties of the microspheres are retained after their ingestion by the fish.

control microspheres were retained in the GI tract of the organism, even though they were squeezed along the tract by the ingestion action and the peristaltic movement of the fish gut. Fig. 6 shows typical bright-field and dark-field optical microscope images of the Japanese medaka, cultured on petri dishes with a suspension of pH-responsive R3 photonic microspheres for 24 h. Close-up inspection of the photonic microspheres along the GI tract of the fish revealed interesting photonic band-gap phenomena that microspheres located at the front part of the GI tract have diffracted green light, while those in the rear part diffracted indigo light (Fig. 7).

O. latipes is a freshwater fish species that do not have a stomach and pylorus [26]. The oesophagus is connected directly to the mid-gut, which like those in many other teleost fish species, coils into loops. No acid digestion of food takes place in stomachless teleostei. The mid-gut is believed to be the major site for food digestion and absorption. Enzymes produced by the pancreas, intestinal wall, bile and the liver are responsible for the breakdown of proteins, lipids and carbohydrates in food. In most teleostei, the optimal pH for these enzymes to function is alkaline (pH 7–9). *In vivo* imaging by the colloidal crystalline photonic microspheres revealed the looped morphology of part the mid-gut of live *O. latipes* that has not been blocked from view by the other abdominal organs. The characteristic green diffraction (with RGB value: R: 102, G: 227, B: 124) of the microspheres in the mid-gut indicated a

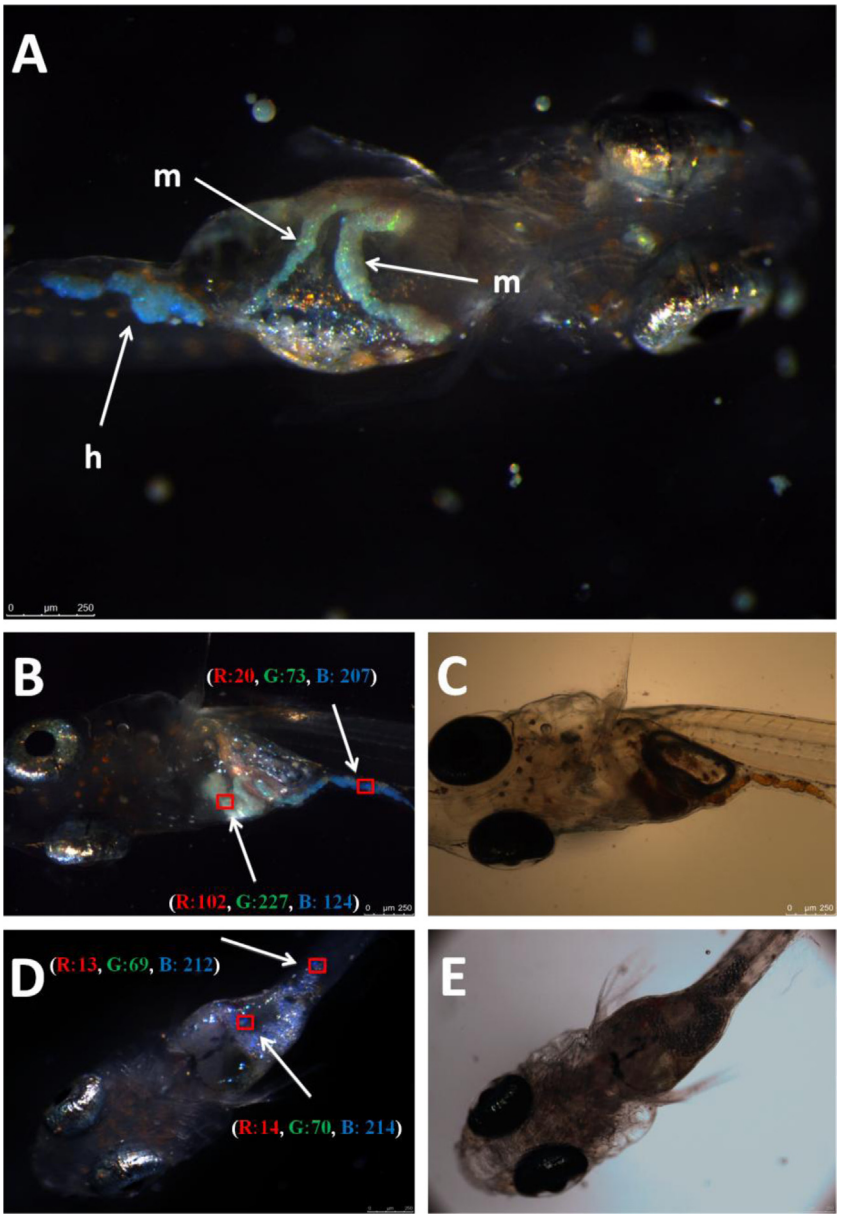

Fig. 7. *In vivo* imaging of the GI tract of live Japanese medaka (*Oryzias latipes*) by the colloidal crystalline microspheres (R3 microspheres) showing the morphology of the looped mid-gut (m) and the hind-gut (h), and the pH of the microenvironment along the GI tract. The dark-field images (A and B) of individual fish clearly show the pH photonic band-gap responses of the microspheres. The upper images (A–C) were obtained using pH-responsive colloidal crystalline microspheres, while the lower images (D and E) were obtained using control microspheres that do not possess pH-responsive properties. (C) and (E) The corresponding bright-field images of B and D respectively.

lumenal pH of >5. Freshwater teleostei are able to absorb sodium ions through their GI tract. Thus, ionic strength inside the gut of freshwater fish is expected to be low. Taking this into account, the green diffraction from the photonic microspheres in the lumen of the mid-gut of *O. latipes* may be correlated to a pH of 8–9 (Fig. 4A and B). The mid-gut is connected to the hind-gut, which is often not well defined in term of gross anatomy, before opening into the anus. The hind-gut is mostly lined by mucus cells instead of the other secretory cells producing digestive enzymes. It has been reported that pH of hind-gut in herbivorous teleost fishes can be lower (in the range of pH 6–7) than that of the mid-gut [27], perhaps due to the absence of pH regulation mechanism necessary for the functioning of digestive enzymes. Results of our *in vivo* imaging revealed that photonic microspheres located in the posterior part of the GI tract of *O. latipes* show well-defined indigo colour diffraction (with RGB value: R: 20, G: 73, B: 207) that is distinctly different from that in the mid-gut. This helps to demarcate the onset of the hind-gut. The indigo colour diffraction also indicates that lumenal pH in this part of the GI tract in live Japanese medaka can, indeed, be acidic (pH 4–5). This suggests that some other metabolic processes may be operating in the hind-gut of the fish. *In vivo* imaging using control photonic colloidal crystalline microspheres fabricated from core–shell nano-sized particles without any acrylic acid moiety in their hydrogel coating revealed a monotonic photonic Bragg diffraction colour throughout the entire length of GI tract.

The fact that photonic band-gap properties of both the pH-responsive and control microspheres were retained within the GI tract indicated that they were structurally intact under the peristaltic squeezing of the intestine of the organism. Even after passing through the GI tract, the excreted microspheres still retained their orderly packed structure and photonic properties (Fig. 8).

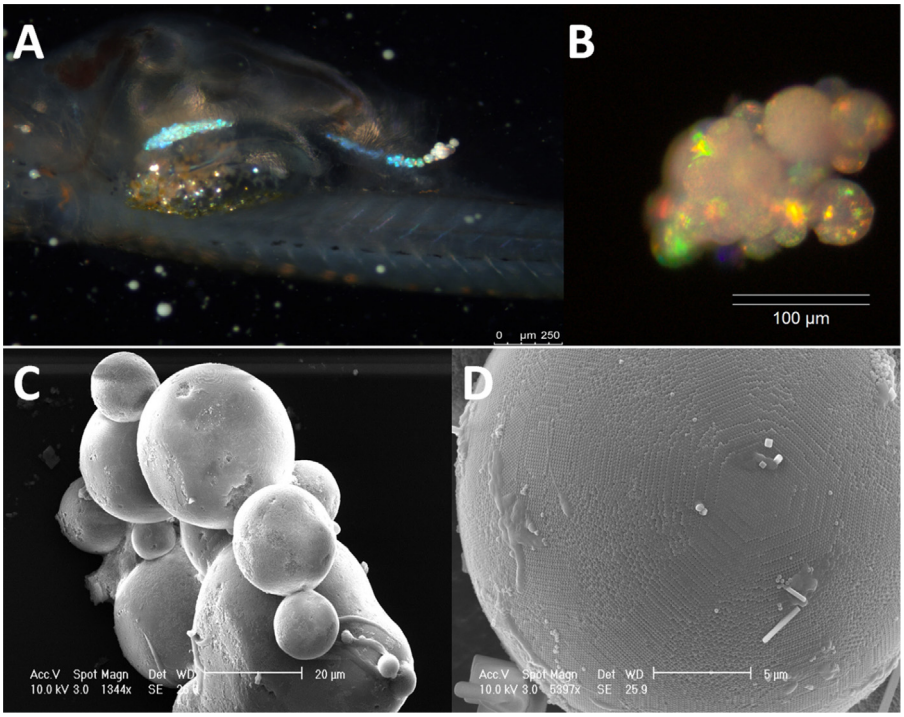

Fig. 8. The dark-field images (A and B) illustrate a live Japanese medaka (*Oryzias latipes*) excreting the colloidal crystalline microspheres, showing the dynamic change in the diffraction colour of the photonic microspheres from hind-gut (h) to external environment. The SEM images (C and D) show the morphology of the colloidal crystalline microspheres excreted by Japanese medaka (*Oryzias latipes*), demonstrating the structural integrity of the colloidal crystalline microspheres for *in vivo* imaging under conditions as harsh as the peristaltic movement of the gut.

4. Conclusion

Unlike molecular probes, functionalized nanoparticles and quantum dots, the inherent size of photonic band-gap materials renders them inappropriate for *in vitro* uses. Yet, they can still be useful in various other bio-imaging applications. In this work, we demonstrated the potential of stimuli-responsive photonic band-gap microspheres in tissue-/organ-level *in vivo* bio-imaging. The versatility of photonic band-gap microspheres facilitates the exploration of many new initiatives in bio-imaging. For example, the pH response range of the photonic colloidal crystalline microspheres in this work might be further tuned by the use of other acidic or basic functional moieties instead of carboxylate, *e.g.* substituents with phosphonate, phenolate or amine/aniline functionalities, in the hydrogel coating of the nano-sized particles composing the colloidal crystalline lattices. In fact, the ease of introduction of a variety of functional moieties to the photonic microspheres allows convenient and rapid development and modification of imaging tools to suit different diagnostic purposes. The use of bio-compatible materials for the construction of these microspheres can offer much safer bio-imaging tools to be used on human. The ability of fine-tuning the photonic band-gap properties of this type of imaging tools by merely altering the size of their nano-sized particles enables the development of imaging probes can work in the near infrared (NIR) spectral region without the need of any specific, and potentially toxic, chemical dyes. The control of the overall size of these microspheres to be less than 3 μm in diameter (about the size of thrombocytes) *via* various advanced fabrication processes should allow these microspheres to be used as imaging tools for blood vessels. All in all, potentials of this type of colloidal crystalline microspheres with stimuli-responsive photonic band-gap properties for bio-imaging warrant further exploration.

Acknowledgements

This work is supported by a research grant #7002882 from the City University of Hong Kong. Mr. Xuemin Du acknowledges the National Natural Science Foundation of China (Nos. 51073146, 51103143, 51173175), and the Joint PhD Scheme of the University of Science & Technology of China and City University of Hong Kong. Special thank is given to Dr. Doris Au of the Department of Biology & Chemistry, City University of Hong Kong, for the provision of Japanese medaka embryos and larvae.

References

[1] (a) R. Weissleder, U. Mahmood, Radiology 219 (2001) 316;
(b) A.S.K. Dzik-Jurasz, Brit. J. Radiol. 76 (2003) S98;
(c) R.Y. Tsien, Nat. Rev. Mol. Cell Biol. (2003) SS16.
[2] (a) J.G. Fujimoto, Nat. Biotechnol. 21 (2003) 1361;
(b) V. Ntziachristos, C. Bremer, R. Weissleder, Eur. Radiol. 13 (2003) 195;
(c) M. Villiger, J. Goulley, E.J. Martin-Williams, A. Grapin-Botton, T. Lasser, Curr. Pharm. Des. 16 (2010) 1595;
(d) B.W. Pogue, F. Leblond, V. Krishnaswamy, K.D. Paulsen, Am. J. Roentgenol. 195 (2010) 321.
[3] (a) B. Ballou, L.A. Ernst, A.S. Waggoner, Curr. Med. Chem. 12 (2005) 795;
(b) R. Bizzarri, M. Serresi, S. Luin, F. Beltram, Anal. Bioanal. Chem. 393 (2009) 1107;
(c) K.K. Maiti, U.S. Dinish, C.Y. Fu, J.-J. Lee, K.-S. Soh, S.W. Yun, R. Bhuvaneswari, M. Olivo, Y.-T. Chang, Biosens. Bioelectron. 26 (2010) 398;
(d) V. Biju, T. Itoh, M. Ishikawa, Chem. Soc. Rev. 39 (2010) 3031;
(e) L. Wang, C. Li, J. Mater. Chem. 21 (2011) 15862.
[4] (a) A. Minta, J.P.Y. Kao, R.Y. Tsien, J. Biol. Chem. 264 (1989) 8171;
(b) R. Weissleder, C.-H. Tung, U. Mahmood, A. Bogdanov, Nat. Biotechnol. 17 (1999) 375;
(c) M. Kamiya, H. Kobayashi, Y. Hama, Y. Koyama, M. Bernardo, T. Nagano, P.L. Choyke, Y. Urano, J. Am. Chem. Soc. 129 (2007) 3918;
(d) B.A. Smith, W.J. Akers, W.M. Leevy, A.J. Lampkins, S. Xiao, W. Wolter, M.A. Suckow, S. Achilefu, B.D. Smith, J. Am. Chem. Soc. 132 (2010) 67;
(e) S. Luo, E. Zhang, Y. Su, T. Cheng, C. Shi, Biomaterials 32 (2011) 7127;
(f) S. Sumalekshmy, C.J. Fahrni, Chem. Mater. 23 (2011) 483.

[5] (a) X. Michalet, F.F. Pinaud, L.A. Bentolila, J.M. Tsay, S. Doose, J.J. Li, G. Sundaresan, A.M. Wu, S.S. Gambhir, S. Weiss, Science 307 (2005) 538;
(b) J. Liu, S.K. Lau, V.A. Varma, R.A. Moffitt, M. Caldwell, T. Liu, A.N. Young, J.A. Petros, A.O. Osunkoya, T. Krogstad, B. Leyland-Jones, M.D. Wang, S. Nie, ACS Nano 4 (2010) 2755;
(c) M. Chakraborty, S. Jain, V. Rani, Appl. Biochem. Biotechnol. 165 (2011) 1178;
(d) A.M. Coto-Garcia, E. Sotelo-Gonzalez, M. Fernandez-Arguelles, R. Pereiro, J.M. Costa-Fernandez, A. Sanz-Medel, Anal. Bioanal. Chem. 399 (2011) 29;
(e) H. Koo, M.S. Huh, J.H. Ryu, D.-E. Lee, I.-C. Sun, K. Choi, K. Kim, I.C. Kwon, Nano Today 6 (2011) 204;
(f) C. Bouzigues, T. Gacoin, A. Alexandrou, ACS Nano 5 (2011) 8488;
(g) Y. Li, C. Jing, L. Zhang, Y.-T. Long, Chem. Soc. Rev. 41 (2012) 632;
(h) M. Mahmoudi, V. Serpooshan, S. Laurent, Nanoscale 3 (2011) 3007.
[6] (a) A.S. Thakor, J. Jokerst, C. Zavaleta, T.F. Massoud, S.S. Gambhir, Nano Lett. 11 (2011) 4029;
(b) J.A. Barreto, W. O'Malley, M. Kubeil, B. Graham, H. Stephan, L. Spiccia, Adv. Mater. 23 (2011) H18.
[7] (a) R. Alford, H.M. Simpson, J. Dubeman, G.C. Hill, M. Ogawa, C. Regino, H. Kobayashi, P.L. Choyke, Mol. Imaging 8 (2009) 341;
(b) S. Ghaden, B. Ramesh, A.M. Seifalian, J. Drug Target 19 (2011) 475;
(c) J.P.M. Almeida, A.L. Chen, A. Foster, R. Drezek, Nanomedicine 6 (2011) 815.
[8] (a) J.H. Holtz, S.A. Asher, Nature 389 (1997) 829;
(b) S.H. Park, B. Gates, Y. Xia, Adv. Mater. 11 (1999) 462;
(c) A. Cho, Science 299 (2003) 1684;
(d) Z. Wu, D. Lee, M.F. Rubner, R.E. Cohen, Small 3 (2007) 1445;
(e) A.-H. Lu, E.L. Salabas, F. Schüth, Angew. Chem. Int. Ed. 46 (2007) 1222;
(f) A.C. Arsenault, D.P. Puzzo, I. Manners, G.A. Ozin, Nat. Photon. 1 (2007) 468;
(g) M. Honda, T. Seki, Y. Takeoka, Adv. Mater. 21 (2009) 1801;
(h) J. Ge, Y. Yin, Angew. Chem. Int. Ed. 50 (2011) 1492.
[9] (a) H.J. Adrogue, N.E. Madias, New Engl. J. Med. 338 (1998) 26;
N. Raghunand, X. He, R. van Sluis, B. Mahoney, B. Baggett, C.W. Taylor, G. Paine-Murrieta, D. Roe, Z.M. Bhujwalla, R.J. Gillies, Brit. J. Cancer 80 (1999) 1005;
(c) R.J. Gillies, N. Raghunand, M.L. Garcia-Martin, R.A. Gatenby, IEEE Eng. Med. Biol. Mag. 23 (2004) 57.
[10] (a) S.E. Day, M.I. Kettunen, F.A. Gallagher, D.E. Hu, M. Lerche, J. Wolber, K. Golman, J.H. Ardenkjaer-Larsen, K.M. Brindle, Nat. Med. 13 (2007) 1382;
(b) Y. Urano, D. Asanuma, Y. Hama, Y. Koyama, T. Barrett, M. Kamiya, T. Nagano, T. Watanabe, A. Hasegawa, P.L. Choyke, H. Kobayashi, Nat. Med. 15 (2009) 104;
(c) J.Y. Ko, S. Park, H. Lee, H. Koo, M.S. Kim, K. Choi, I.C. Kwon, S.Y. Jeong, K. Kim, D.S. Lee, Small 6 (2010) 2539.
[11] (a) K. Lee, S.A. Asher, J. Am. Chem. Soc. 122 (2000) 9534;
(b) C.E. Reese, M.E. Baltusavich, J.P. Keim, S.A. Asher, Anal. Chem. 73 (2001) 5038;
(c) H. Saito, Y. Takeoka, M. Watanabe, Chem. Commun. (2003) 2126;
(d) J. Wang, Y. Cao, Y. Feng, F. Yin, J. Gao, Adv. Mater. 19 (2007) 3865;
(e) K. Matsubara, M. Watanabe, Y. Takeoka, Angew Chem. Int. Ed. 46 (2007) 1688;
(f) X. Hu, J. Huang, W. Zhang, M. Li, C. Tao, G. Li, Adv. Mater. 20 (2008) 1.
[12] (a) O.D. Velev, A.M. Lenhoff, E.W. Kaler, Science 287 (2000) 2240;
(b) A.D. Dinsmore, M.F. Hsu, M.G. Nikolaides, M. Marquez, A.R. Bausch, D.A. Weitz, Science 298 (2002) 1006;
(c) V. Rastogi, S. Melle, O.G. Calderón, A.A. García, M. Marquez, O.D. Velev, Adv. Mater. 20 (2008) 4263;
(d) J. Ge, H. Lee, J. Kim, Z. Lu, H. Kim, J. Goebi, S. Kwon, Y. Yin, J. Am. Chem. Soc. 131 (2009) 15687.
[13] (a) O.D. Velev, K. Furusawa, K. Nagayama, Langmuir 12 (1996) 2374;
(b) V.N. Manoharan, A. Imhof, J.D. Thorne, D.J. Pine, Adv. Mater. 13 (2001) 447;
(c) J.H. Moon, G.R. Yi, S.M. Yang, D.J. Pine, S.B. Park, Adv. Mater. 16 (2004) 605;
(d) H.Y. Li, H.Q. Wang, A.H. Chen, B. Meng, X.Y. Li, J. Mater. Chem. 15 (2005) 2551;
(e) D.M. Kuncicky, K. Bose, K.D. Costa, O.D. Velev, Chem. Mater. 19 (2007) 141;
(f) J.H. Jang, D. Dendukuri, T.A. Hatton, E.L. Thomas, P.S. Doyle, Angew. Chem. Int. Ed. 46 (2007) 9027.
[14] K.P. Velikov, O.D. Velev, in: B.P. Binks, T.S. Horozov (Eds.), Colloidal Particles at Liquid Interfaces, University Press, Cambridge, UK, 2006, pp. 225–297.
[15] (a) M.K. Yoo, Y.M. Sung, C.S. Cho, Polymer 41 (2000) 5713;
(b) X. Zhou, L. Wenig, Q. Chen, J. Zhang, D. Shen, Z. Li, M. Shao, J. Xu, Polym. Int. 52 (2003) 1153;
(c) V. Kozlovskaya, E. Kharlampieva, M.L. Mansfield, S.A. Sukhishvili, Chem. Mater. 18 (2006) 328.
[16] (a) P.J. Flory, Principles of Polymer Chemistry, Cornell University Press, Ithaca, NY, 1953;
(b) T. Tanaka, Phys. Rev. Lett. 40 (1978) 820;
(c) F. Horkay, I. Tasaki, P.J. Basser, Biomacromolecules 1 (2000) 84.
[17] Z.-Z. Gu, H. Chen, S. Zhang, L. Sun, Z. Xie, Y. Ge, Colloids Surf. A 302 (2007) 312.
[18] R.C. Hardman, D.C. Volz, S.W. Kullman, D.E. Hinton, Anat. Record Adv. Integr. Anat. Evol. Biol. 290 (2007) 770.
[19] R. Mayoral, J. Requena, J.S. Moya, C. Lopez, A. Cintas, H. Miguez, F. Meseguer, L. Vazquez, M. Holgado, A. Blanco, Adv. Mater. 9 (1997) 257.
[20] B.W. Gamer, T. Cai, S. Ghosh, Z. Hu, A. Neogi, Appl. Phys. Exp. 2 (2009) 057001.
[21] J.F.J. Dippy, S.R.C. Hughes, A. Rozanski, J. Chem. Soc. (1959) 2492.
[22] (a) J. Hasa, M. Ilavsky, K.J. Dusek, Polym. Sci. Polym. Phys. 13 (1975) 253;
(b) M. Ilavsky, Polymer 22 (1981) 1687;
(c) T. Çaykara, U. Bozkaya, Ö. Kantoğlu, J. Polym. Sci. B 41 (2003) 1656.
[23] (a) F.P. Ojeda, C.W. Cáceres, Mar. Ecol. Prog. Ser. 118 (1995) 37;
(b) M. Yúfera, M.J. Darías, Aquaculture 267 (2007) 94;
(c) C.M. Wood, C. Bucking, M. Grosell, J. Exp. Biol. 213 (2010) 2681;
(d) L. Márquez, R. Robles, G.A. Morales, F.J. Moyano, Fish Physiol. Biochem. 38 (2012) 859;
(e) E.S.M. Carvalho, S.F. Gregório, D.M. Power, A.V.M. Canário, J. Fuentes, J. Comp. Physiol. B 182 (2012) 1069.
[24] (a) H.W. Detrich, M. Westerfield, L.I. Zon (Eds.), The Zebrafish: Biology, Academic Press, San Diego, 1999;
(b) Y. Ishikawa, Bioessays 22 (2000) 487;
(c) J. Wittbrodt, A. Shima, M. Scharti, Nat. Rev. Genet. 3 (2002) 53;
(d) M. Kinoshita, Medaka: Biology, Management and Experimental Protocols, Wiley-Blackwell, Ames, IA, 2009.
[25] I. Rønnestad, R.P. Domingues, M. Tanaka, Fish Physiol. Biochem. 22 (2000) 225.
[26] D. Kobaysahi, T. Jinbo, K. Naruse, H. Takeda, Dev. Growth Differ. 48 (2006) 283.
[27] E.A. Sturm, M.H. Horn, Mar. Biol. 132 (1998) 515.